Continuous Aperture Phased MIMO: A New Architecture for Optimum Line-of-Sight Links

Akbar M. Sayeed
Elect. & Comp. Engineering
University of Wisconsin
Madison, WI 53706
Email: akbar@engr.wisc.edu

Nader Behdad
Elect. & Comp. Engineering
University of Wisconsin
Madison, WI 53706
Email: behdad@engr.wisc.edu

***Abstract*—We propose a new communication architecture – continuous aperture phased MIMO – that combines the elements of MIMO, continuous aperture antennas, and phased arrays, for achieving the capacity of line-of-sight (LoS) links. CAP-MIMO is based on a hybrid analog-digital transceiver architecture that employs a novel antenna array structure – a high-resolution discrete lens array – to enable a continuous aperture phased-MIMO operation with a low-complexity analog-digital interface. Our focus is on millimeter-wave (60-100GHz) LoS links for high-rate (1-100Gb/s) applications. We propose a framework for modeling and analyzing a LoS link in beamspace, discuss the key elements of the CAP-MIMO system, and present results on its significant capacity advantages over two state-of-the-art designs: i) systems that employ continuous aperture "dish" antennas for high power efficiency but no spatial multiplexing gain, and ii) MIMO systems that use discrete antenna arrays for multiplexing gain but suffer in power efficiency.**

I. Introduction

Millimeter (mm) wave communication systems, operating in the 60-100GHz band, are emerging as a promising technology for meeting the increasing demands on wireless capacity. In addition to offering large bandwidths, a key advantage of mm-wave systems is that they offer high-dimensional MIMO operation with relatively compact antenna arrays. However, unlike the original motivation for MIMO in rich multipath environments, the recent interest in mm-wave MIMO systems is mainly focussed on high-rate (1-100 Gb/s) communication over line-of-sight (LoS) links due to the quasi-optical propagation characteristics at mm-wave frequencies. Two design approaches dominate the state-of-the-art: i) traditional systems, which we refer to as DISH systems, that employ continuous aperture "dish" antennas for high power efficiency but no spatial multiplexing gain (e.g., the technology available from Bridgewave Communications); and ii) MIMO systems that use discrete antenna arrays for a higher multiplexing gain but suffer from poor power efficiency; see, e.g., [1].

This paper proposes a new wireless transceiver architecture – continuous aperture phased MIMO – that combines the elements of MIMO, continuous aperture antennas, and phased arrays for achieving the capacity of line-of-sight (LoS) links.[1] CAP-MIMO is based on a *hybrid analog-digital architecture* that employs a novel antenna array structure – *a high-resolution discrete lens array (DLA)* [2] – to enable a *quasi-continuous aperture* phased-MIMO operation. The DLA-based analog-digital interface performs analog beamforming and offers a low-complexity/low-cost alternative to *high-dimensional* phased arrays that employ digital beamforming. In particular, in the context of gigabit LoS links, CAP-MIMO combines the power gain of DISH systems and multiplexing gain of MIMO systems to deliver very significant capacity gains.

The basic mathematical framework for CAP-MIMO leverages the connection between MIMO systems and phased uniform linear arrays (ULAs) from a communication perspective that was first established in [3]. The CAP-MIMO framework is applicable to a very broad class of scenarios: short-range versus long-range, LoS versus multipath propagation, point-to-point versus network links. However, our focus is on mm-wave, high-rate (1-100 Gbps) LoS links, which could either be short-range (as in high-rate indoor applications, e.g. HDTV) or long-range (as in wireless backhaul). The DLA-based architecture also enables point-to-multipoint network operation that is not possible with existing designs.

Starting with an overview in the next section, Sections III-V present the key elements of the CAP-MIMO system for LoS links with one-dimensional (1D) linear aperture antennas. The DLA-based low-dimensional analog-digital interface is discussed in Sec. V. Sec. VI presents results on capacity advantages of CAP-MIMO over the state-of-the-art designs. For details on the mathematical development, including extensions to 2D apertures, we refer the reader to [4]. **A note on notation:** Lowercase boldfaced letters (e.g., $\mathbf{h}$) denote complex-valued column vectors and uppercase boldfaced letters denote matrices (e.g, $\mathbf{H}$). $\mathrm{tr}(\mathbf{H})$ denotes the trace and $\mathbf{H}^H$ the complex conjugate transpose of $\mathbf{H}$.

II. Overview of the CAP-MIMO Framework

Fig. 1 depicts a 1D LoS link in which the transmitter and receiver antennas have a linear aperture of length A and are separated by a distance $R \gg A$. Let $\lambda_c = c/f_c$ denote the wavelength of operation, where c is the speed of light and f_c is the carrier frequency. For $f_c \in [60, 100]$GHz, $\lambda_c \in [3, 5]$mm. For a given LoS link characterized by the physical parameters (A, R, λ_c) the CAP-MIMO framework

[1]The authors would like to acknowledge the Wisconsin Alumni Research Foundation and the National Science Foundation for supporting this work.

addresses the following fundamental question: **What is the link capacity at any operating signal-to-noise ratio (**SNR**)?** The CAP-MIMO theory characterizes this fundamental limit [4] and the DLA-based realization of the CAP-MIMO system is aimed at approaching this limit.

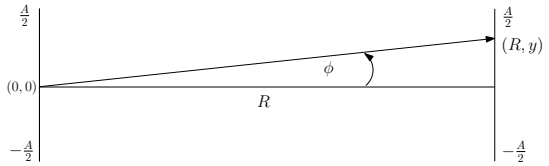

Fig. 1. The LoS channel.

From a communication perspective, the continuous aperture antennas can be equivalently represented by critically sampled (virtual) n-dimensional ULAs with spacing $d = \lambda_c/2$ where

$$n = \frac{A}{d} = \frac{2A}{\lambda_c} \tag{1}$$

is a fundamental quantity associated with a linear aperture antenna: The analog spatial signals transmitted or received by the antennas belong to an n-dimensional signal space. We term n the *maximum number of* **analog (spatial) modes** *supported by the antennas*. Viewing the apertures as critically sampled ULAs, the LoS link in Fig. 1 can be equivalently represented by an $n \times n$ MIMO system [3], [4]

$$\mathbf{r} = \mathbf{H}\mathbf{x} + \mathbf{w} \tag{2}$$

where $\mathbf{x}$ is the the n-dimensional transmitted signal vector, $\mathbf{r}$ is the received signal vector, $\mathbf{w}$ is the (white Gaussian) noise vector, and $\mathbf{H}$ is the $n \times n$ channel matrix. The fundamental limits of the LoS link are governed by the singular values of $\mathbf{H}$. As we elaborate later, $\mathbf{H}$ exhibits $p_{max} \ll n$ dominant non-zero singular values due to LoS propagation. We term p_{max} as the *maximum number of* **digital (spatial) modes** *supported by the LoS link*. That is, the information bearing signals in the LoS link lie in a p_{max}-dimensional subspace of the n-dimensional spatial signal space. p_{max} is a fundamental quantity related to the *LoS link* and can be calculated as (see (7))

$$p_{max} \approx \frac{A^2}{R\lambda_c} \ . \tag{3}$$

Fig. 2 shows a (complex baseband) schematic of a DLA-based hybrid analog-digital architecture for the CAP-MIMO system. At the transmitter, p independent digital data streams, $1 \le p \le p_{max}$, corresponding to the digital modes, serve as the input vector $\mathbf{x}_e$ $(x_e(i), i = 1, \cdots, p)$. For each symbol,

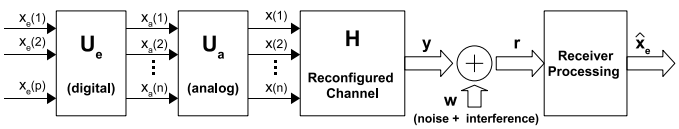

Fig. 2. The hybrid analog-digital architecture of CAP-MIMO.

$\mathbf{x}_e$ is digitally transformed by the $n \times p$ matrix $\mathbf{U}_e$ to yield the vector $\mathbf{x}_a = \mathbf{U}_e\mathbf{x}_e$. As elaborated later, only a subset of elements of $\mathbf{x}_a$, on the order of p_{max}, are non-zero, which (after upconversion and symbol pulse generation; not shown in Fig. 2) serve as the analog signals that excite appropriately placed feed elements on the focal surface of the DLA. The (analog) operation of the DLA is represented by the $n \times n$ matrix $\mathbf{U}_a$ induced by the location of the feed elements and the critical sampling of the aperture. The n-dimensional signal vector $\mathbf{x} = \mathbf{U}_a\mathbf{x}_a$ represents the (critically sampled) analog spatial signal radiated by the transmitter aperture. For a perfectly designed DLA, $\mathbf{U}_a$ is an $n \times n$ discrete Fourier transform (DFT) matrix. At the receiver, the analog signals on the aperture are first processed by a DLA. Again, on the order of p_{max} sensors on the focal surface of the DLA will carry most of signal energy. These signals are downconverted, sampled, and digitally processed to recover an estimate, $\hat{\mathbf{x}}_e$ of the transmitted signal vector $\mathbf{x}_e$.

III. Communication Through Spatial Beams

The n spatial modes can be associated with n orthogonal beams that cover the entire (one-sided) spatial horizon ($-\pi/2 \le \phi \le \pi/2$ in Fig. 1) as illustrated in Fig. 3(a). Each of these beams can carry an independent data stream. However, due to the finite apertures and large distance $R \gg A$, only a small number of modes/beams, $p_{max} \ll n$, couple from the transmitter to the receiver, and vice versa, as illustrated in Fig. 3(b). The low-dimensionality of LoS links can be exploited by CAP-MIMO for simultaneously sending multiple data streams to multiple receivers, as illustrated in Fig. 3(c).

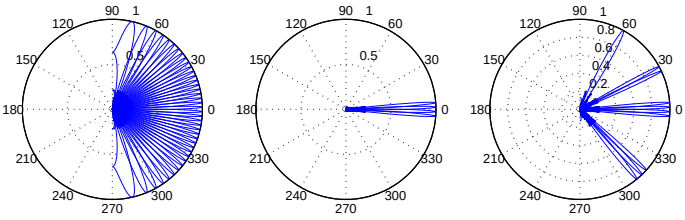

Fig. 3. CAP-MIMO beampatterns: $n = 40$, $p_{max} = 4$. (a) n orthogonal beams covering the entire spatial horizon. (b) p_{max} beams that couple the finite aperture antennas. (c) point-to-multipoint communication.

The n-dimensional signal spaces, associated with the transmitter and receiver, can be described via appropriately chosen steering and response vectors [3]. We use the following convention for the set of (symmetric) indices for describing a signal vector of length n: $\mathcal{I}(n) = \{i - (n-1)/2 : i = 0, \cdots, n-1\}$. We define the *spatial frequency* θ that is related to angle ϕ as [3]: $\theta = \frac{d}{\lambda_c}\sin(\phi) = 0.5\sin(\phi)$. An n-dimensional array response/steering vector, $\mathbf{a}(\theta)$, represents a plane-wave phase front associated with a point source in the direction θ and its elements are given by

$$a_i(\theta) \ = \ e^{-j2\pi\theta i} \ , \ \ i \in \mathcal{I}(n) \tag{4}$$

representing a discrete complex sinusoid, with frequency θ, over the sampled aperture. Note that $\mathbf{a}(\theta)$ are periodic in θ with period 1 and two different steering/response vectors are

orthogonal if their frequencies are separated by a multiple of $\Delta\theta_o = 1/n$, which is a measure of the *spatial resolution* or the *beamwidth* associated with an n-element phased array [3], [4]. As a result, an orthogonal basis for the n-dimensional signal space can be generated by uniformly sampling $\theta \in [-1/2, 1/2]$ with spacing $\Delta\theta_o$. In fact,

$$\mathbf{U} = \frac{1}{\sqrt{n}}[\mathbf{a}(\theta_i)]_{i\in\mathcal{I}(n)} \quad , \quad \theta_i = i\Delta\theta_o = \frac{i}{n} \tag{5}$$

is a (unitary) DFT matrix with $\mathbf{U}^H\mathbf{U} = \mathbf{U}\mathbf{U}^H = \mathbf{I}$. For critical $\lambda_c/2$ sampling, the columns of $\mathbf{U}$ represent orthogonal spatial beams that cover the entire range of $\phi \in [-\pi/2, \pi/2]$, as illustrated in Fig. 3(a).

IV. The LoS Channel: Coupled Orthogonal Beams

We consider beamspace representation of $\mathbf{H}$ [3], [4]. First note that in Fig. 1 any point y on the transmitter array represents a plane wave impinging on the receiver array from the direction $\phi \approx \sin(\phi) \approx \frac{y}{R}$. We thus get the following correspondence between the critically sampled points on the transmitter array and the angles subtended at the receiver array [4]: $y_i = i\frac{\lambda_c}{2} \Longleftrightarrow \theta_i = 0.5\sin(\phi_i) \approx \frac{y_i}{2R} = i\frac{\lambda_c}{4R}$, $i \in \mathcal{I}(n)$. The n columns of $\mathbf{H}$ are given by $\mathbf{a}(\theta)$ for these θ_i

$$\mathbf{H} = [\mathbf{a}_n(\theta_i)]_{i\in\mathcal{I}(n)} \quad , \quad \theta_i = i\Delta\theta_{ch} = i\frac{\lambda_c}{4R} \ . \tag{6}$$

We define the channel power as $\sigma_c^2 = \mathrm{tr}(\mathbf{H}^H\mathbf{H}) = n^2$.

The LoS link capacity is directly related to the rank of $\mathbf{H}$ which is in turn related to the number of orthogonal beams, p_{max}, that couple the transmitter and the receiver, as illustrated in Fig. 3. The number p_{max} can be calculated as

$$p_{max} = \frac{2\theta_{max}}{\Delta\theta_o} = 2\theta_{max}n \approx \frac{A^2}{R\lambda_c} \tag{7}$$

where $\theta_{max} = 0.5\sin(\phi_{max})$ denotes the one-sided *spatial bandwidth*, $\sin(\phi_{max}) \approx \frac{A}{2R}$, and ϕ_{max} denotes the (one-sided) angular spread of the signals subtended by the transmitter array at the receiver array, and vice versa. We note that p_{max} in (7) is a fundamental link quantity that is independent of the virtual antenna spacing, d, used in our analysis.

The beamspace channel representation, $\mathbf{H}_b$, clearly reveals this lower-dimensional channel structure [3]

$$\mathbf{H} = \mathbf{U}\mathbf{H}_b\mathbf{U}^H \Leftrightarrow \mathbf{H}_b = \mathbf{U}^H\mathbf{H}\mathbf{U} \tag{8}$$

where $\mathbf{U}$ is the (unitary) DFT matrix which also represents operation of a perfectly designed DLA. Fig. 4 shows a zoomed-in contour plot of the absolute values of $\mathbf{H}_b$ for a short-range 80GHz link with $n = 80$ and $p_{max} = 2$. As evident, while $\mathbf{H}_b$ is an $n \times n$ matrix, only a (nearly diagonal) sub-matrix $\tilde{\mathbf{H}}_b$ of approximate size $p_{max} \times p_{max}$ is non-zero, indicating that all of the channel power is concentrated in p_{max}-dimensional subspaces at the transmitter and receiver.

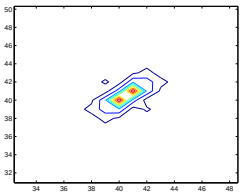

Fig. 4. Contour plot of the beamspace channel matrix $\mathbf{H}_b$.

V. Optimal Signaling: Low-Complexity Hybrid Analog-Digital Interface

Communication theory tells us that transmission and reception over the singular vectors of $\mathbf{H}$ is optimal for achieving capacity. The transformed channel matrix is diagonal, representing *non-interfering* channels over which independent data streams can be communicated. As evident from the near-diagonal nature of $\mathbf{H}_b$ in Fig. 4, the DFT matrix $\mathbf{U}$ serves as a good approximation to the singular vectors. Furthermore, a subset of p_{max} DFT basis vectors enables access to the communication subspace. Since an ideal DLA affects a DFT, $\mathbf{H}_b$ (with a $p_{max} \times p_{max}$ non-zero sub-matrix $\tilde{\mathbf{H}}_b$), represents the ideal channel matrix coupling the focal arc feeds of the transmitter and receiver DLAs. Since the digital-to-analog (D/A) interface occurs between the output of $\mathbf{U}_e$ and the input to $\mathbf{U}_a$ (DLA) in Fig. 2, this means that a CAP-MIMO transmitter (or receiver) has a D/A (or A/D) interface of complexity of p_{max}, enabled by *analog beamforming* performed by the DLA. In contrast, a conventional phased array-based system with *digital beamforming* will have an A/D (D/A) interface of complexity n across the array elements. Exact channel diagonalization can be realized via a p_{max}-dimensional singular value decomposition (SVD) of $\tilde{\mathbf{H}}_b$ (rather than an n-dimensional SVD of $\mathbf{H}$ in a phased-array system) and using the singular vectors in the digital transform $\mathbf{U}_e$ in Fig. 2.

The analog transform $\mathbf{U}_a$ Fig. 2 is a critically sampled representation of the *analog spatial transform* between the focal surface and the continuous aperture of the DLA. With an appropriately designed DLA *aperture phase profile*, this spatial transform can accurately approximate a DFT; $\mathbf{U}_a \approx \mathbf{U}$. CAP-MIMO is based on a high-resolution DLA to approximate a continuous-aperture operation. Fig. 5 provides a comparison

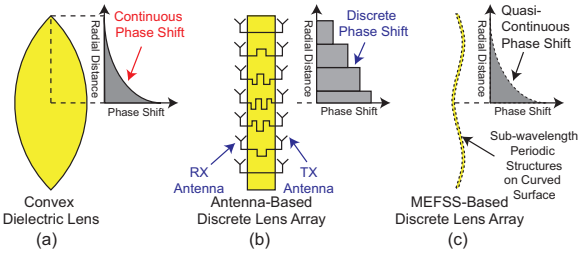

Fig. 5. (a) a dielectric lens. (b) a traditional microwave lens. (c) a high-resolution DLA composed of sub-wavelength pixels.

between a double convex dielectric lens, a conventional microwave lens composed of arrays of receiving and transmitting antennas connected through transmission lines of variables lengths (see, e.g., [5], [6]), and a high-resolution DLA [2].

A high-resolution DLA is composed of a number of spatial phase shifting elements, or pixels, distributed on a flexible membrane. The pixels are ultra-thin and their dimensions are extremely small, e.g. $0.05\lambda_c \times 0.05\lambda_c$ as opposed to $\lambda_c/2 \times \lambda_c/2$ in conventional DLAs, enabling a high-resolution aperture phase profile design. These high-resolution DLAs have other unique advantages, including large field of views of $\pm 70^\circ$ and extremely wide bandwidths [2]. The CAP-MIMO theory also suggests a new approach to DLA phase profile design that will be reported elsewhere.

VI. Capacity Comparison with State-of-the-Art

We next present closed-form expressions that provide accurate approximations for the capacity of the CAP-MIMO, DISH and MIMO systems for a 1D LoS link depicted in Fig. 1. For details and exact capacity analysis see [4].

1) CAP-MIMO System: The CAP-MIMO system achieves the capacity of a LoS link with given n and p_{max}. It is well-known in antenna theory that the array/beamforming gain of a linear aperture A is proportional to $n = 2A/\lambda_c$. This gain is achieved at the both the transmitter and receiver ends. However, for a given p_{max}, while the entire aperture is exploited at the transmitter side for each beam, only a fraction $1/p_{max}$ of the aperture is associated with a beam on the receiver side (see Fig. 3). As a result, the total transmit-receiver array/beamforming gain associated with each beam or data stream is n^2/p_{max} – the average of the p_{max} non-zero eigenvalues of the transmit covariance matrix $\mathbf{H}^H\mathbf{H}$. Distributing the total transmit SNR ρ over these p_{max} modes yields the following closed-form approximation for the capacity of the CAP-MIMO system at any ρ

$$C_{c-mimo}(\rho) \approx p_{max} \log\left(1 + \rho \frac{n^2}{p_{max}^2}\right) . \qquad (9)$$

2) Conventional DISH System: A DISH system transmits a single data stream. Thus, the CAP-MIMO capacity formula (9) for $p = p_{max} = 1$ gives the capacity for an *optimized* DISH system in which the link is adjusted so that $p_{max} = 1$. If $p_{max} > 1$, then the capacity of a DISH system is given by

$$C_{dish}(\rho) = \log(1 + \rho\lambda_{max}) \qquad (10)$$

where λ_{max} is the largest eigenvalue of $\mathbf{H}^H\mathbf{H}$ that satisfies $n^2/p_{max} \le \lambda_{max} \le n^2$.

3) Conventional MIMO System: A conventional MIMO system with a multiplexing gain p_{mimo} uses p_{mimo} antennas with (Rayleigh) spacing $d_{ray} = \sqrt{\frac{R\lambda_c}{p_{mimo}}}$ to create p_{mimo} orthogonal channels [1], [4]. Assuming omnidirectional antennas, the capacity of the MIMO system is given by

$$C_{mimo}(\rho) = p_{mimo} \log(1 + \rho) . \qquad (11)$$

If higher gain antennas are used, the capacity expression can be modified by using a higher effective ρ. For $p_{max} = p_{mimo}$, the loss in SNR in a MIMO system compared to the CAP-MIMO system can be attributed to the grating lobes/beams due to larger than critical antenna spacing ($d_{ray} \approx \frac{n}{p_{max}}\lambda_c/2$) [3], [4]. The grating lobes also result in increased interference and reduced security.

4) Numerical Results: We note that p_{max}, defined in (7) is a baseline indicator of the rank of the channel matrix $\mathbf{H}$. The effective rank, p_{eff}, depends on the number of dominant eigenvalues of $\mathbf{H}^H\mathbf{H}$ and and is typically in the range $p_{eff} \in [\lceil p_{max} \rceil, \lceil p_{max} + 1 \rceil]$ [4]. In both cases presented next, $p_{max} = p_{mimo} = 2$ whereas $p_{eff} = 3$.

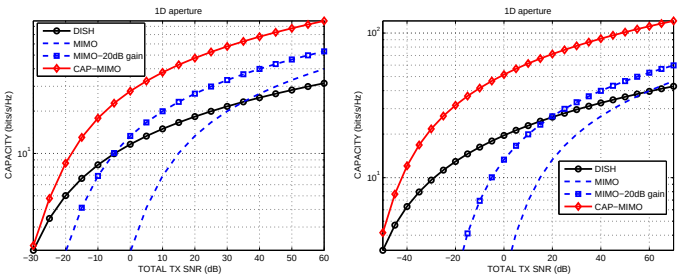

(a) Short-range link (b) Long-range link

Fig. 6. Capacity comparison for: (a) a short-range ($R = 3$m) 1D link at 80 GHz, (b) long-range ($R = 1$km) 1D link at 60 GHz.

Fig. 6(a) compares the capacity of MIMO, DISH and CAP-MIMO systems for a short-range ($R = 3m$) link operating at $f_c = 80$ GHz with linear aperture $A = 15$cm corresponding to a MIMO system with $p_{mimo} = 2$ and $d_{ray} = 7.5cm$. Critically sampled continuous aperture of the same size yields $n = 80$ and $p_{max} = 2$ for the CAP-MIMO and DISH systems. There are $p_{eff} \approx 3$ dominant eigenvalues of $\mathbf{H}^H\mathbf{H}$ and the CAP-MIMO capacity is accurately approximated by (9) with p_{eff} substituted for p_{max}. As evident, between the two conventional systems, MIMO dominates at high SNRs whereas DISH dominates at low SNRs. CAP-MIMO on the other hand, combines the attractive features of DISH (high power/antenna gain) and MIMO (multiplexing gain) to exceed the performance of both conventional systems over the entire SNR range. Fig. 6(b) compares the three systems for a long-range ($R = 1$km) 60GHz link with linear aperture $A = 3.16$m corresponding to $p_{mimo} = 2$ ($d_{ray} = 1.58$m), $p_{max} = 2$ ($p_{eff} = 3$), and $n = 1265$. The performance gains of CAP-MIMO over DISH and MIMO are even more pronounced in this case. We note that performance gains of CAP-MIMO are even more pronounced for 2D apertures [4].

References

[1] E. Torkildson, B. Ananthasubramaniam, U. Madhow, and M. Rodwell, "Millimeter-wave MIMO: Wireless links at optical speeds," *Proc. Allerton Conference*, Sep. 2006.

[2] M. A. Al-Joumayly and N. Behdad, "Design of conformal, high-resolution microwave lenses using sub wavelength periodic structures," in *2010 IEEE Antennas and Propagation Society/URSI Symposium*, Toronto, ON, July 11-17 2010.

[3] A. M. Sayeed, "Deconstructing multi-antenna fading channels," *IEEE Trans. Signal Processing*, vol. 50, no. 10, pp. 2563–2579, Oct. 2002.

[4] A. Sayeed and N. Behdad, "Continuous aperture phased mimo: Basic theory and applications," *Proc. Allerton Conference*, Sep. 2010.

[5] W. Shiroma, E. Bryeron, S. Hollung, and Z. Popovic, "A quasi-optical receiver with angle diversity," in *Proceedings of the IEEE International Microwave Symposium*, San Francisco, CA, 1996, pp. 1131–1135.

[6] D. T. McGrath, "Planar three-dimensional constrained lens," *IEEE Trans. Antennas Propagat.*, vol. 34, no. 1, p. 4650, Jan. 1986.